OPTO-ELECTRONICS REVIEW **13**(4), 269–279

Molecular engineering of triphenylene-based discotic liquid crystal conductors

R.J. BUSHBY*[1], K.J. DONOVAN[2], T. KREOUZIS[2], and O.R. LOZMAN[1]

[1]Centre for Self Organising Molecular Systems (SOMS), University of Leeds, Woodhouse Lane, LS2 9JT Leeds, United Kingdom
[2]Queen Mary and Westfield College, University of London, Mile End Road, E1–4NS London, United Kingdom

2,3,6,7,10,11-hexakis(hexyloxy)triphenylene (HAT6) gives a columnar hexagonal mesophase between 70 and 100°C and a hole mobility of 7.1×10^{-4} $cm^2V^{-1}s^{-1}$. Two methods are compared for extending the mesophase range to encompass the operationally-significant room temperature range and for enhancing the charge-carrier mobility: introduction of a lateral nuclear dipole and formation of a CPI (complementary polytopic interaction) 'compound'. Introduction of two fluorine substituents into the nucleus of HAT6 gives 1,4-difluoro-2,3,6,7,10,11-hexakis(hexyloxy)triphenylene (2F-HAT6). This has a lateral nuclear dipole and gives a columnar hexagonal mesophase from below room temperature to 121°C whereas the CPI mixture of 2F-HAT6 with 2,3,6,7,10,11-hexakis(4-nonylphenyl)triphenylene (PTP9) has a columnar mesophase from below room temperature to 129°C. At 100°C the time-of-flight hole mobilities of these two systems are increased to 1.6×10^{-3} $cm^2V^{-1}s^{-1}$ for 2F-HAT6 and 1.5×10^{-2} $cm^2V^{-1}s^{-1}$ for the CPI compound 2F-HAT6 + PTP9.

Keywords: liquid crystal, semi-conductor, time-of-flight, photoconduction, hole mobility, molecular engineering.

1. Introduction

The great advances made by organic synthesis in the last few decades mean that it is now relatively easy to engineer the bulk properties of organic molecular materials by refinement of the molecular structure. In the liquid crystal field this capability has been exploited for many years in the area of display applications but liquid crystals are now beginning to excite interest as semiconductors [1,2]. Relative to crystalline or amorphous semi-conductors, liquid crystals have the advantages of good processability, self-healing, anisotropy, and spontaneous alignment. The columnar phases of discotic liquid crystals have been likened to an array of self-aligning molecular wires (Fig. 1). The stacked aromatic nuclei provide a graphite-like conducing pathway along the columns while an annulus of mobile disordered alkyl side-chains insulates each column from its neighbours. Although commercial applications have yet to be developed, applications have been suggested in xerographic copiers, laser printers [3], photovoltaic devices, electroluminescent devices [4], FETS and many other areas [5]. However, to realize such dreams we need mesophases that persist down to room temperature. Triphenylene derivatives illustrate this problem. Triphenylenes are the most synthetically accessible discogens and the only discogens currently made on a commercial scale [6] but none of the simple 2,3,6,7,10,11-hexa-*n*-alkoxytriphenylenes give columnar phases that persist down to room temperature [7]. The most straightforward ways of extending the range over which the columnar phases of a discotic liquid crystals is stable are by introducing a lateral dipole into the aryl core [8] or by introducing branching into the side-chain [9] or by forming a non-covalent CPI (complementary polytopic interaction) 'compound' [10,11]. A nuclear dipole is believed to stabilize the columnar structure through an anti-ferroeletric correlation of dipoles along the column as shown in Fig. 2 (left) [8] and in CPI compounds the columnar structure is stabilized by interlocking alternating large and small discs (Fig. 2, right). From the standpoint of improving the conductivity both of these approaches have the additional benefit that potentially they can also increase the charge-carrier mobility whereas branching of the side-chains is likely to disorder the columnar structure and decrease the mobility.

In this paper, the effect of a nuclear dipole is explored using the example of the new triphenylene derivative 1,4-difluoro-2,3,6,7,10,11- hexakishexyloxytriphenylene, 2F-HAT6 (**1a**) (Fig. 3) and the effect of CPI 'compound' formation using the 1:1 mixture formed between (**1a**) and 2,3,6,7,10,11-hexakis(4-nonylphenyl)triphenylene (PTP9 **3a**). In both cases the columnar structure is stabilized, columnar phases are obtained that persist down to room temperature and the time-of-flight hole mobilities are enhanced relative to the 'parent' discogen, 2,3,6,7,10,11-hexakis(hexyloxy)triphenylene HAT6 (**2b**).

*e-mail: richardb@chem.leeds.ac.uk

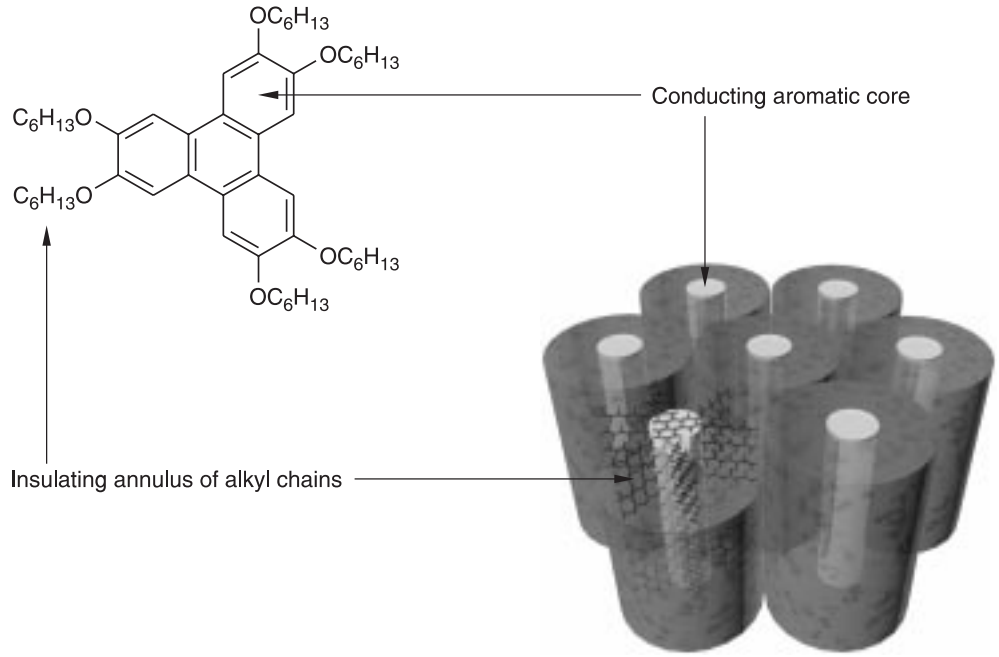

Fig. 1. Schematic representation of the Col_h phase of a triphenylene-based discotic liquid crystal HAT6 (**2a**).

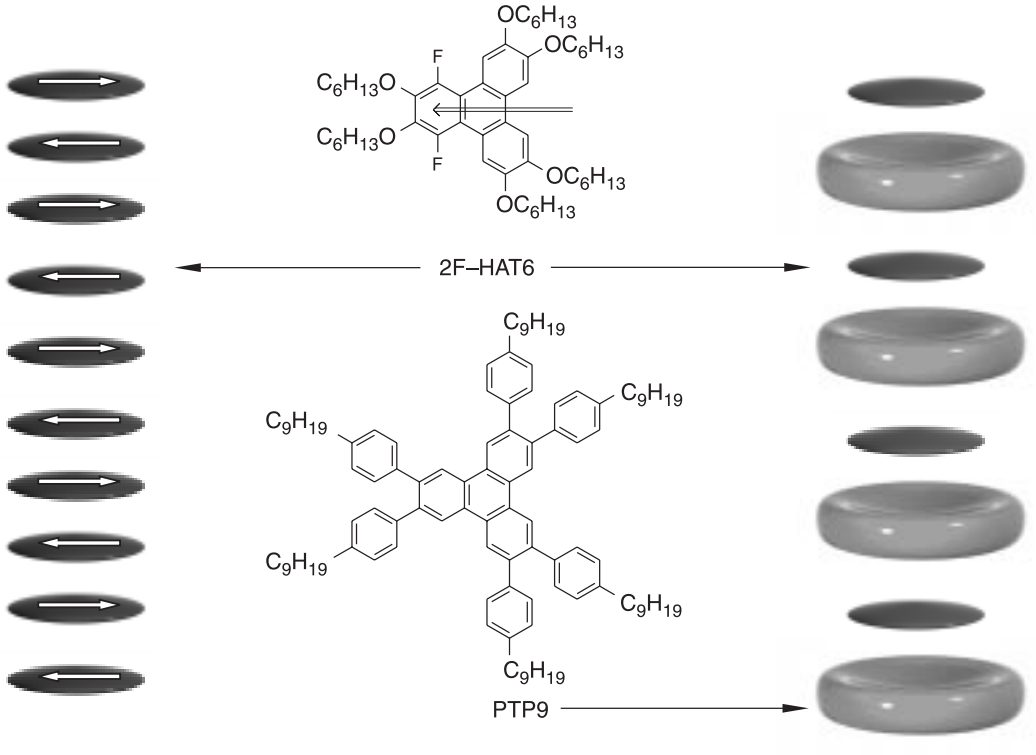

Fig. 2. Schematic representation of the stabilization of a columnar phase through antiferroelectric alignment of molecular dipoles as in 2F-HAT6 (**1a**) or by formation of a CPI compound as in 2F-HAT6 (**1a**) + PTP9 (**3a**).

2. Results and discussion

2.1. Synthesis and phase behaviour

The synthesis of 2F-HAT6 (**1a**) is summarized in Schemes 1 and 2. The key intermediate is 1,4-difluoro-2,3- dialkoxybenzene (**8**). This was synthesized from commercially available 2,5-difluorophenol (**4**) by the route shown in Scheme 1 [12]. Initial attempts to synthesize 2F-HAT6 (**1a**) directly by intermolecular oxidative coupling of 3,4,3',4'-tetraalkoxybiphenyl and 1,4-difluoro-2,3-dialkoxybenzene (**8**) with $FeCl_3$/DCM (Scheme 2) [13–15], failed to produce the required product. The successful alternative, shown in Scheme 2, used

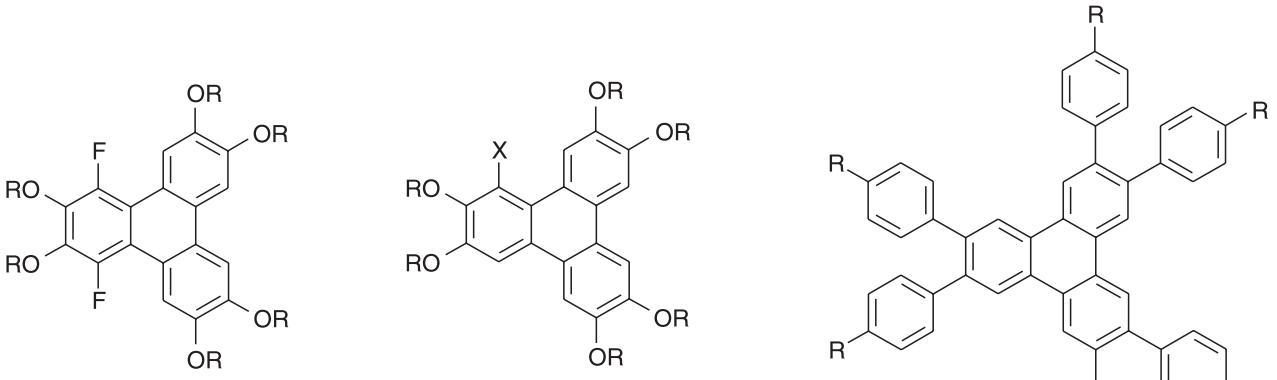

1a R = C_6H_{13}, 2F–HAT6
1b R = CH_3, 2F–HAT1

2a R = C_6H_{13}, X = H. HAT6
2b R = C_6H_{13}, X = NO_2. NO_2–HAT6
2c R = CH_3, X = H. HAT1
2d R = CH_3, X = NO_2. NO_2–HAT1
2e R = C_2H_5, X = NO_2. NO_2–HAT2

3a R = C_9H_{19}, PTP9
3b R = CH_3, PTP1

Fig. 3. Molecular structures of the materials discussed in this paper.

Scheme 1. Synthesis of 1,4-difluoro-2,3-dihexyloxybenzene (**8**, R = C_6H_{13}) and 1,2-dibromo-3,6-difluoro-4,5-dihexyloxybenzene (**9**, R = C_6H_{13}). (i): RBr/ K_2CO_3/EtOH/ reflux, 77% (ii): 1. BuLi/THF/–78°C, 2. $B(OMe)_3$/THF/–78°C, 3. 1M HCl(aq), (iii): H_2O_2, 82% (iv): RBr/ K_2CO_3/EtOH/ reflux, 80% (v): Br_2/DCM/0°C–25°C, 98%.

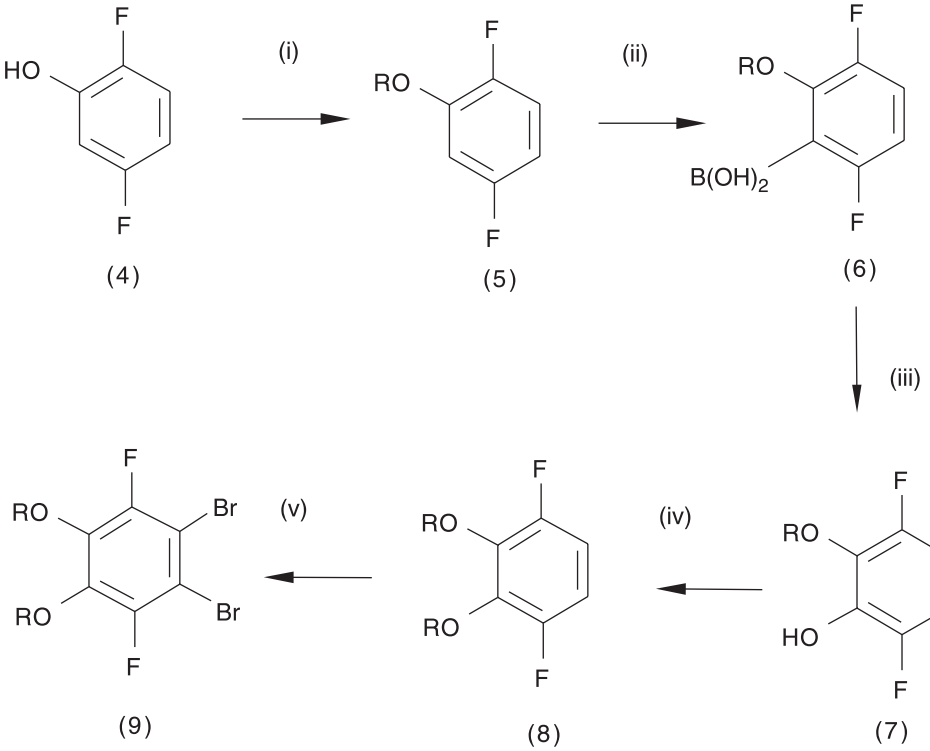

Suzuki coupling of boronic ester (**10**) with 1,2-dibromo-3,6-difluoro-4,5-dihexyloxybenzene (**9**) to give the substituted ortho-terphenyl (**11**) (Scheme 2) [16]. The ortho-terphenyl (**11**) was then oxidized using iron (III) chloride in dichloromethane, followed by a reductive methanol workup [15] to produce 2F-HAT6 (**1a**), isolated yields in excess of 90% (Scheme 2). The reactions all scale-up easily and batches of 2F-HAT6 greater than 1 g have been successfully prepared. The ease of purification of the product is worthy of note and it was found that repeated column chromatography and recrystallization were not necessary.

Differential scanning calorimetry (DSC) and optical polarizing microscopy (OPM) were used to characterize the phase behaviour (Table 1). 2F-HAT6 (**1a**) has a wider mesophase range than HAT6, (**2a**). It clears at a higher temperature and no Cr-Col transition is detected down to –30°C.

A thin film of 2F-HAT6 (**1a**) was prepared by compressing a melted sample between glass slides. The shear-

Scheme 2. Top, direct oxidative coupling of (**8**) with tetralkoxybiphenyl failed to produced the required product. Bottom, Suzuki coupling of 1,2-dibromo-3,6-difluoro-4,5-dihexyloxybenzene (**9**) with pinacol-(3,4-dihexyloxybenzene) boronic ester (**10**) produces the ortho-terphenyl (**11**). Subsequent $FeCl_3$/DCM mediated oxidative coupling produces 2F-HAT6 (**1a**). R = C_6H_{13} (i): 0.3 mol% $Pd(PPh_3)_4/C_6H_5CH_3/H_2O/Na_2CO_3$/Ar, 80%. (ii): 1. $FeCl_3$/DCM, 2. MeOH > 90%.

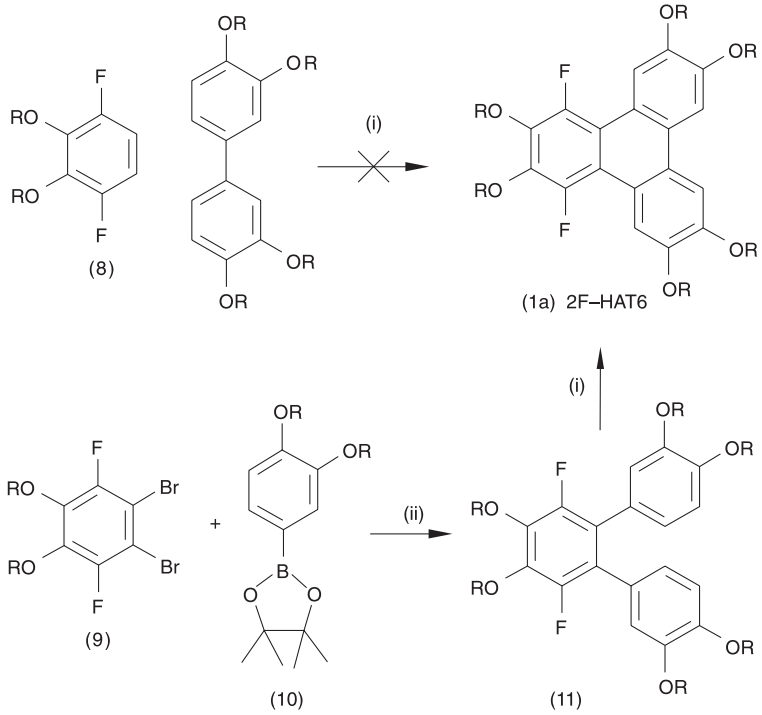

Table 1. Summary of the transitions [T/°C, (ΔH/kJmol^{-1})] of 2F-HAT6 (**1a**), HAT6 (**2a**), HAT6-NO_2 (**2b**), and PTP9 (**3a**) and the CPI 'compounds'. The values were determined by DSC and OPM and the phases were assigned on the basis of OPM observations and X-ray diffraction experiments.

Material	Phase behaviour °C (J/g)	
	Alone	CPI 'compound' with PTP9 (**3a**)
2FHAT6 (**1a**)	Col_h 121.2 (13) I[a]	Col 129.3 (16) I[a]
HAT6 (**2a**)[7]	Cr 69.5 (48) Col_h 99.5 (7) I	Col_h 155 (19) I[a]
NO_2-HAT6 (**2b**)[8,36]	Col_h 137 (8) I[a]	Cr 100 I[b]
PTP9 (**3a**)[14]	Cr_1 70.9 (34)[c] Cr_2 81.1 (var)[d] I	–

[a]No other transitions down to –30°C (the lowest temperature tested).
[b]Enthalpies variable due to the immiscibility of the materials.
[c]Observed on second and subsequent heating only.
[d]Transition observed on first heating only.

ing force that this produces causes the molecules to align in a planar manner with the columns parallel to the plane of the glass substrate and OPM shows the resultant sample to be birefringent and highly disordered. Upon heating into the isotropic liquid (> 122°C) and slowly cooling, there is a first order isothermal transition into the Col_h phase, and the predominant orientation of the Col_h phase formed is homeotropic: with the columns forming perpendicular to the surface.

When the sample is cooled at 10°Cmin^{-1} these homeotropic domains are large and a single homeotropic monodomain is formed when the cooling rate is 5°Cmin^{-1}. Figure 4(A) shows the optical texture of 2F-HAT6 (**1a**) after a single annealing cycle at a cooling rate of 10°Cmin^{-1}. An equimolar mixture of 2F-HAT6 (**1a**) with PTP9 (**3a**), forms a non-covalent CPI compound with a slighter higher clearing temperature and enthalpy than 2F-HAT6 (**1a**) alone (Table 1). Upon cooling from the melt, the liquid crystalline phase initially forms with the molecules aligned in a planar fashion; crystallizing from the melt as dendrites [Figs. 4(B) and 4(C)]. These quickly grow to cover the sample but, after as little as five minutes, these realign and a homeotropically aligned film is obtained, Fig. 4(D).

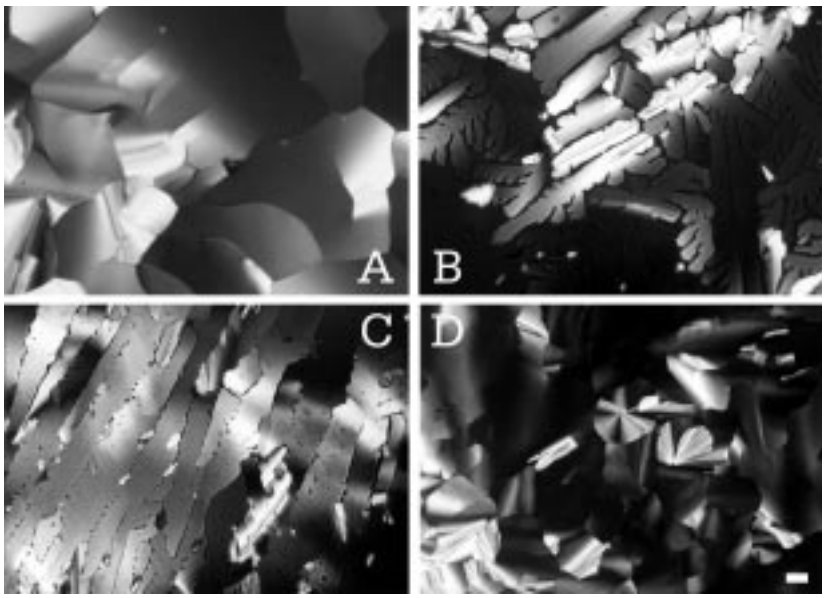

Fig. 4. Optical texture of 2F-HAT6 (**1a**) as viewed through crossed-polarizing filters after cooling from the isotropic liquid at 10°C min^{-1} (100°C) (A). Dendrites form initially when an isotropic 1:1 mixture of 2F-HAT6 (**1a**) + PTP9 (**3a**) is cooled to 120°C at 10°C min^{-1} and held at this temperature (B). As Fig. 2(B) as the dendrites coalesce a few seconds later (C) and (D) as Fig. 2(C) after annealing for five minutes at 120°C a large homeotropic monodomain forming. Scale bar (bottom right) = 100 μm for all figures.

2.2. Molecular modelling of the CPI 'compound'

When a triphenylene-based discotic liquid crystal and PTP9 (**3a**) are mixed in a 1:1 stoichiometric ratio, a non- covalent CPI 'compound' is often formed. This exhibits properties that are entirely different to those of the individual components [10,11,17]. In the case of the 1:1 mixture of HAT6 (**2a**) and PTP9 (**3a**), for example, the melting point of the 1:1 mixture is much higher than that of either of the individual components. The X-ray diffraction patterns of such CPI mixtures show extra reflections and sharper diffraction maxima than those observed in either individual component. However, unlike the diffraction patterns obtained for the plastic [18] and helical phases [19], there are no peaks that can be unambiguously assigned as arising out from a three dimensionally ordered structure. The HAT and PTP molecules form an alternating stack (Fig. 3) which is more ordered than that formed by the HAT component on its own and this generally leads to higher mobilities. Clearly there is some sort of attractive interaction between the two molecules but this is not of the net quadrupole/net quadrupole or charge-transfer type. We have modelled the interaction using a simple molecular mechanics force-field with added terms to account for the interaction of pi-electrons (the XED, extended electron distribution force field) [17]. The attractive interaction actually arises out of favourable van der Waals and coulombic interactions across many sites of intermolecular contact giving a complementary many-site (polytopic) interaction (CPI). The XED modelling package has now been used to investigate the interactions of PTP with HAT6 (**2a**), 2F-HAT6 (**1a**) and NO_2-HAT6 (**2b**) and the results are summarized in Table 2.

Table 2. Results of XED docking of HAT and PTP molecules showing the van der Waals and coulombic contributions to the total energy of the pair of molecules in the lowest energy configuration. The numbers underlined in brackets are the predicted energies for CPI compound formation, ΔE. ΔE is calculated as the difference between the energy of the heterodimer and the mean of the two homodimer energies [Eq. (1)]. A negative value of ΔE indicates that a stabilizing interaction is occurring between the molecules.

Material	Energy (kcal mol^{-1})		
	VDW's	Coulombic	Total
2FHAT1 (**1b**) + 2FHAT1 (**1b**)	–33. 6	–2.4	–35.9
HAT1 (**2c**) + HAT1 (**2c**)	–37.4	–2.4	–39.8
NO_2-HAT1 (**2d**) + NO_2-HAT1 (**2d**)	–25.2	–10.7	–35.9
PTP1 (**3b**) + PTP1 (**3b**)	–45.9	9.7	–36.2
2FHAT1 (**1b**) + PTP1 (**3b**)	–40.8 (–1.1)	–1.6 (–5.3)	–42.4 (–6.4)
HAT1 (**2c**) + PTP1 (**3b**)	–43.8 (–2.1)	–6.2 (–9.8)	–49.9 (–11.8)
NO_2-HAT1 (**2d**) + PTP1 (**3b**)	–32.6 (+3.0)	–2.0 (–1.5)	–34.5 (+1.5)

Table 3. Summary of time-of-flight hole mobilities for HAT6 (**2a**) and 2F-HAT6 (**1a**) and their CPI 'compounds' with PTP9 (**3a**).

Material	Temperature (°C)	Phase	Mobility ($cm^2V^{-1}s^{-1}$)
2FHAT6 (**1a**)	25	Col_h	1.6×10^{-3}
HAT6 (**2a**)[21]	70	Col_h	7.1×10^{-4}
2FHAT6 (**1a**) + PTP9 (**3a**)	25	Col_h	1.5×10^{-2}
HAT6 (**2a**) + PTP9 (**3a**)[37]	40	(Col)Glass	1.39×10^{-2}

To minimize computation time and to try to understand the 'pi-stacking' component, the side-chains have been reduced to methyl groups. In contrast to HAT6 (**2a**), 2F-HAT6 (**1a**) and NO_2-HAT6 (**2b**) have net dipoles, rather than a net quadrupole as the lowest non-zero terms of their multipole expansions. The single crystal X-ray structure of NO_2-HAT2 (**2e**) shows that the molecules pack in such a way as to maximize the dipolar interaction between adjacent disks (Fig. 5). The dipole moment for HAT2-NO_2 (**2e**) is estimated as μ~6 Debye and is almost parallel to the direction of the carbon-nitrogen bond [8]. In 2F-HAT1 (**1b**), the two fluorine groups are opposed across the triphenylene ring, producing a small dipole (μ~1 Debye) in the plane of the nucleus and perpendicular to a line drawn between the fluorine atoms. In agreement with the experimental results the XED calculations predict that the net interaction between PTP1 and HAT1 and between PTP1 and 2F-HAT1 are favourable but that between PTP1 and NO_2-HAT1 is not. The force field programme allows these difference to be understood in terms of the partitioning of the interaction energy between VDW and Coulombic terms (Table 2). The HAT derivatives are all predicted to have a favourable coulombic interaction with PTP1 (**3b**), although the size of this is reduced as the dipole moment on the HAT component increases. When HAT1 (**2c**) is docked with a PTP1 (**3b**) molecule the energy minimum is located with the HAT1 (**2c**) centrally above or below the triphenylene nucleus of PTP1 (**3a**) (Fig. 6, left). As also shown schematically in Fig. 3, the peripheral phenyl substituents on the PTP nucleus create a 'dish-like' hollow into which the HAT fits. The program also predicts that, when 2F-HAT1 (**1b**) is docked with PTP1 (**3b**) the minima are located a little off-centre (Fig. 6, centre) so as to exploit the quadrupolar interactions of the peripheral phenyl substituents of the PTP with the dipole of the HAT. In NO_2-HAT, the dipole moment is much larger and the HAT component seems to finds it increasingly difficult to find a suitable location that will compensate for the dipole moment. Furthermore, the α-nitro substituent in NO_2-HAT1 (**2d**) introduces steric hindrance. The combination of these two factors produces a minimum energy heterodimer structure in which the components are widely displaced and often tilted with respect to each other. The VDW's term suffers because of the lack of core-core overlap and the mixture of NO_2-HAT1 (**2d**) and PTP1 (**3a**) is correctly predicted to be unstable (see Tables 1 and 2). The prediction of off-central stacking for 2F-HAT1 is interesting. It does not seem to greatly affect the overall energy of the pair or to prevent CPI compound formation.

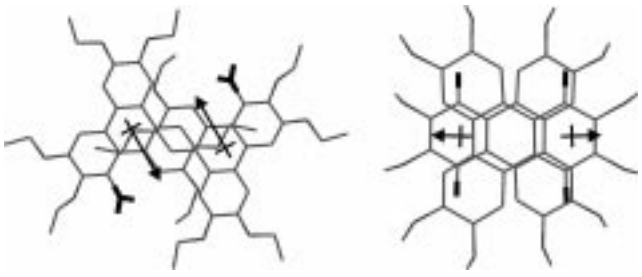

Fig. 5. Left, shows the geometry of a pair of NO_2-HAT2 molecules taken from the single crystal structure. Right, shows the geometry of a pair of 2F-HAT1 (**1b**) molecules calculated using the XED dock routine. Dipole moments, calculated at the PM3 level are represented by the arrows. Both homodimers are viewed parallel to the tertiary inertial axis.

2.3. Time-of-flight photoconduction

In time-of-flight studies of a homeotropically aligned columnar phase, the carrier mobility along the columns is determined directly from the decay in the current after charge carriers are injected using a short pulse of laser light [20]. In the columnar hexagonal phase of hexaalkoxytriphenylenes, the carrier mobilities are typically low (of the order of 10^{-3} $cm^2V^{-1}s^{-1}$) [21] and almost temperature independent

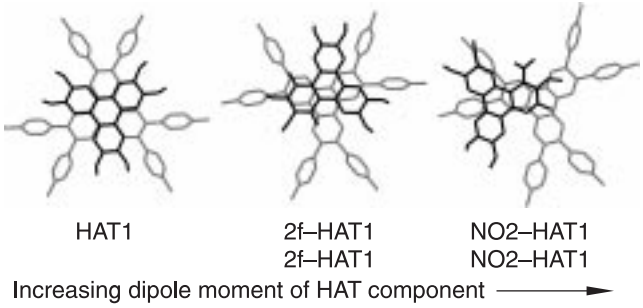

Fig. 6. Left, Minimum energy structure from the XED docking of HAT1 (**2c**) with PTP1 (**3b**). In the majority of the low energy docked structures the HAT1 (**2c**) molecules are located directly over the central triphenylene ring. Centre: Shows the minimum energy structure for docking 2F-HAT1 (**2b**) with PTP1 (**3b**). The dipole introduced by the inclusion of fluorine atoms causes a loss of symmetry. Right: Shows a minimum energy structure for docking NO_2-HAT1 (**2d**) + PTP1 (**3b**). All heterodimers are viewed along the tertiary inertial axis of the pair, the primary and secondary inertial axes being aligned with x and y coordinate axes respectively. The PTP component is shown in grey and the HAT component in black.

[22]. In such low mobility systems, conduction is dominated by a hopping mechanism [23–25] and the mobility is found to depend on the coupling of the polaron to its environment [25], the size of the aromatic core [26], the overlap disc-to-disc [27] but most particularly on the order of the liquid crystal: the correlation length within the column [28]. This is easy to understand. Although the fluid nature of liquid crystals meant that there are no persistent deep traps the number and nature of the short-lived traps and barriers that the charge carrier has to overcome in its passage through the sample depends on the order and the extent of thermal fluctuations. The introduction of a strongly electron withdrawing group such as $–NO_2$, –CN, –F into the core of the discotic molecule stabilizes the columnar phases but in terms of charge carrier mobility it produces two opposing effects. Firstly, the anti-ferroelectric dipole-dipole coupling between adjacent rings (Fig. 3) will increase the correlation length resulting in an increase in the charge carrier mobility but, secondly, the interaction of the hole with surrounding disordered dipoles will increase the dispersion in the hopping times. This latter effect is well known in isotropic amorphous molecular solids where introduction of a molecular dipole is seen to result in an increased spread in hopping times and lower mobilities [29,30]. Good TOF transits were observed for the Col_h phase of 2F-HAT6 (**1a**) and a typical example is shown in Fig. 7. There is a weak temperature dependence of the hole-mobility, which has a maximum value of 1.6×10^{-3} $cm^2V^{-1}s^{-1}$ at 100°C (Fig. 8). In the case of the CPI compound formed between 2FHAT6 (**1a**) and PTP9 (**3a**), the mobility is an order of magnitude greater. The transits appear slightly different in that the long time photocurrent does not decay so rapidly to zero (Fig. 9). The broadening of the TOF transit may be the consequence of the lack of perfect alternating AB columnar structure and the presence of occasional ABB or AAB defects. These are unavoidable. It is impossible to produce mixtures with absolutely exact 1:1 stoichiometry. As in the case of the introduction of a lateral dipole, formation of a CPI 'compound' produces two opposing effects in terms of charge carrier mobility. Firstly, the interlocking of adjacent rings (Fig. 3) will increase the correlation length resulting in an increase in the charge carrier mobility but, secondly, the mismatch in the HOMO/LUMO levels of 2F-HAT6 (**1a**) and PTP9 (**3a**) [31,32] means that the charge carriers need to overcome the barriers presented by the alternating molecules along the column. As in other CPI compounds the first of these two effects seems to be the more important. Once again the mobility is increased relative to the parent system and it is only weakly temperature dependent (Fig. 10).

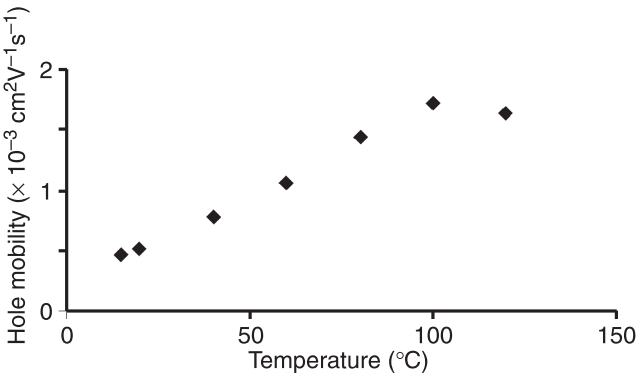

Fig. 8. Temperature dependence of the hole mobility for 2F-HAT6 (**1a**).

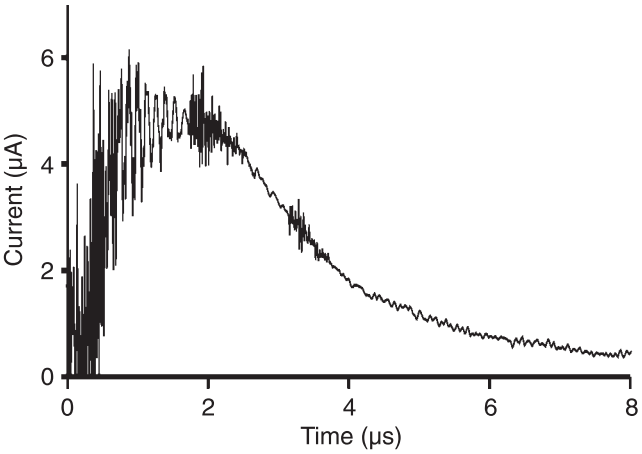

Fig. 9. Typical TOF transit for the 1:1 CPI 'compound' formed by 2FHAT6 (**1a**) and PTP9 (**3a**), voltage = 15 V, temp. = 60°C, and cell spacing = 6.1 μm.

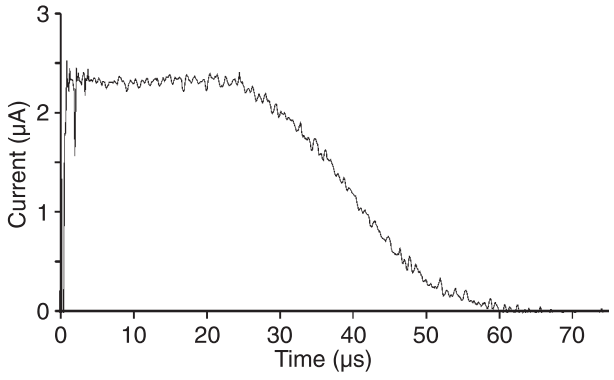

Fig. 7. Typical TOF transit for 2F-HAT6 (**1a**), voltage = 15 V, temp. = 60°C, and cell spacing = 6.7 μm.

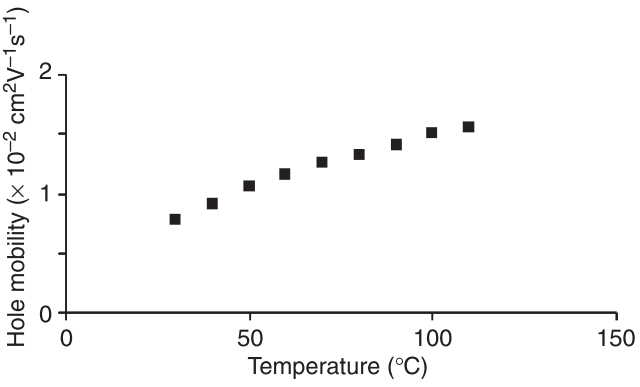

Fig. 10. The variation of hole mobility with temperature for the CPI 'compound' 2F-HAT6 (**1a**) + PTP9 (**3a**).

3. Conclusions

The potential great advantage of organic molecular materials is the opportunities they offer for us to tune bulk properties through refinement of the molecular structure and control over intermolecular interactions. In the case of the hexa-*n*-alkoxytriphenylenes we have shown that the Col_h mesophase range can be extended into the applications-significant room temperature range either by introducing a lateral dipole into the aryl core or by forming a non-covalent CPI (complementary polytopic interaction) compound. The introduction of a lateral dipole through the inclusion of α-substituents has proved a valuable tool for the modulation of the mesophase behaviour of triphenylene-based discotic liquid crystals but bulky groups such as nitro or cyano can also produce problems. For example, in the case of nitro, the nucleus is distorted from planarity and, also for steric reasons, it is found that the nitro- and cyano-substituted triphenylenes do not form CPI compounds with PTP derivatives. However, in this paper we have shown that the introduction of the much smaller α-fluoro substituents generates the desired lateral dipole without such complications. Although the columnar structure can be stabilized either by introducing a lateral dipole into the aryl core or by forming a non-covalent CPI 'compound' and this is not only associated with an increased mesophase range but also an increase in carrier mobility (possibly attributed to an increased correlation length) the later strategy seems generally the more successful particularly in terms of increasing the mobility.

4. Experimental

4.1. Differential scanning calorimetry

Differential scanning calorimetry (DSC) was performed on a Perkin-Elmer 7 thermal analysis system (at a heating and cooling rate of 10°C min^{-1} in sealed Al pans).

4.2. Time-of-flight photoconduction

For the time-of-flight photoconduction experiments the cells were fabricated by evaporating aluminium onto quartz slides making one of them semitransparent and placing the two slides on top of one another, separated by 5 μm PTFE spacers. The cell was held in an aluminium assembly block which was temperature controlled to within ±1°C. The cell was filled by capillary action and the sample was then thermally annealed to produce a monodomain. The cell uniformity and thickness were monitored using interference fringes and measurement of the interference transmission spectrum using a Hitachi U3000 spectrophotometer. A Fluke power supply was used to supply the potential drop across the cell thus applying a uniform electric field along the columnar director.

Using a nitrogen laser at 337 nm with a 6-ns pulse width, photocurrent transients were excited. The light intensity was controlled using neutral density filters in order to keep the photosignal low enough to avoid signal distortion as a result of space charge effects. The photocurrents were detected as a voltage drop across an input resistor to a pre-amplifier in turn delivering the signal to a 50-W terminated Tektronix digitalizing oscilloscope with a 1-ns rise time. The laser emits radio frequency interference, RFI, picked up by the detection apparatus so it is necessary to collect a second baseline signal with no light on the sample. In this way, in post-acquisition processing the RFI was subtracted and the signal greatly cleaned up. White noise was also reduced by signal averaging [33,34].

4.3. Molecular modelling

The geometries of the molecules under investigation were optimized and a conformational search was performed using the XED force field [35] within the COSMIC programme. Finally, the extended pi-electrons and lone pairs were located based on the force-field parameterization and the semi-empirical calculated charge distribution. The general form of the force field and full details of the routines and the XED force-field parameterization are given in the literature [17]. The global minima from the conformational analysis were then docked in pairs using a free SIMPLEX minimizer. This involves holding one of the molecules stationary whilst another molecule (bullet) is moved towards it. This process is then repeated for a total of 250 bullets with different starting positions, which are distributed evenly around the surface of a sphere. The output from the docking experiment gives the overall interaction energy and its VDW's and coulombic contributions. By comparing the interactions between the molecules and themselves (i.e., the homodimers U_{AA} and U_{BB}) with the mixed system (i.e., the heterodimer U_{AB}) it is possible to predict whether or not a stable mixture should be formed. The results are used to quantify this difference in interaction with the term ΔE, defined in equation $\Delta E = U_{AB} - (U_{AA} + U_{BB})/2$. A compound is predicted to form if ΔE carries a negative value.

4.4. Synthesis

4.4.1. General. Nuclear magnetic resonance spectra were recorded on a Bruker DPX300 spectrometer. Microanalyses were carried out at Leeds University Microanalytical Laboratory. All C, H, and N analytical figures are percentage values.

The syntheses of HAT6 and of PTP9 [14] and the methods used to make the CPI compounds [22] have been described elsewhere.

4.4.2. 1,4-Difluoro,2-hexyloxybenzene (5). 2,5-Difluorophenol (**4**, 23 g, 0.172 mol) was dissolved in dry, distilled ethanol (300 ml) under a stream of nitrogen. 1-bromo-

hexane (31.75 g, 0.193 mol, 1.2 eq) and potassium carbonate (133 g, 0.964 mol, 5.5 eq) were added and the reaction mixture was stirred vigorously under reflux for 4 days. Dichloromethane (300 ml) was added to the straw coloured mixture, which was then filtered through a bed of celite to remove the potassium carbonate. The filtrate was washed with water (3×100 ml), and dried with magnesium sulphate. Removal of the solvent *in vacuo* yields 34.07 g of pale brown oil. This was distilled under reduced pressure to yield a colourless oil (29.22 g, 77%), bp 70°C @ 0.7 mmHg; (found: C, 67.35; H, 7.55. $C_{12}H_{16}OF_2$ requires C, 67.3; H, 7.53; O, 7.47; F, 17.76%).

4.4.3. 1,4-Difluoro,2-hexyloxybenzene-1-boronic acid (6). 1,4-Difluoro,2-hexyloxybenzene (**5**, 29.22 g, 0.137 mol) was stirred in THF (150 ml) under anhydrous conditions. The solution was cooled to –78°C under a stream of dry nitrogen and butyl-lithium (1.6 M in hexanes, 81 ml, 0.129 mol) was added drop-wise via cannular over 60 minutes. Stirring was continued for 3 hours at –78°C. The reaction was then quenched (at –78°C over 30 min) with a solution of tri-methylborate (13.23 g, 0.129 mol) in THF (200 ml). The cooling bath was then removed, and the reaction mixture was stirred at room temperature overnight.

Upon addition of HCl (10%, 90 ml) the white suspension dissolved to produce a straw coloured solution. Stirring was continued for 1 hour and then the solvents were removed *in vacuo* at room temperature to yield colourless oil that rapidly formed into white crystals (49 g). These crystals were dissolved in ether (250 ml), washed with water (3×100 ml) and dried with magnesium sulphate. Removal of the solvent yielded white crystals of the title compound (48 g), which were used without further purification.

4.4.4. 3,6-Difluoro,2-hexyloxyphenol (7). White crystals of 1,4-difluoro,2-hexyloxybenzene-1-boronic acid (6, 48 g) were dissolved in warm toluene (150 ml) and hydrogen peroxide (43 ml, 30%) was added drop-wise. Heating was continued for 45 min at 100°C. Once the solution had cooled to room temperature water was added (50 ml) and the layers were separated. The toluene layer was washed with ferrous ammonium sulphate (10%, 2×50 ml) and water (2×50 ml). The combined organic extracts were dried with magnesium sulphate, filtered and the solvent was removed to yield crude 3,6-difluoro,2-hexyloxyphenol (7) as a pale yellow oil (31.67 g, 100%). The crude product was dissolved in toluene (150 ml), extracted with sodium hydroxide solution (10%w/v in methanol, 3×50 ml). The purple, aqueous extract, containing the phenoxide anion of the product, was then re-acidified with concentrated HCl until all of the colour had been displaced (pH~4). The phenol was then extracted with dichloromethane (3×100 ml), washed with water (3×50 ml), dried with magnesium sulphate and filtered. Removal of the solvent *in vacuo* yielded the required product as an orange/brown oil (27.2 g, 87%). Kugelrohr distillation was performed under reduced pressure (2mbar), the colourless distillate collected when the oven temp was 100°C was found to contain only (**4**) (26.5 g, 82%), (Found: C, 62.65; H, 6.9. $C_{12}H_{16}O_2F_2$ requires C, 62.6; H, 6.9; O, 13.91; F, 16.52%).

4.4.5. 1,4-Difluoro-2,3-dihexyloxybenzene (8). 3,6-Difluoro-2-hexyloxyphenol (**7**, 25 g, 0.11 mol) was dissolved in dry, distilled ethanol (350 ml) under a stream of nitrogen. 1-Bromohexane (45.35 g, 0.275 mol, 2.2 eq) and potassium carbonate (75.1 g, 0.54 mol, 5.5 eq) were added and the reaction mixture was stirred vigorously under reflux for 2 days. Dichloromethane (300 ml) was added to the orange reaction mixture, which was then filtered through a bed of celite to remove the potassium carbonate. The filtrate was washed with water (3×100 ml), and dried with magnesium sulphate. Removal of the solvent *in vacuo* yields 24.07 g of pale brown oil. This was distilled under reduced pressure to yield a colourless oil (18.82 g, 80%), bp 102°C, 0.2 mbar; (found: C, 68.8; H, 9.05. $C_{18}H_{28}O_2F_2$ requires C, 68.76; H, 8.98; O, 10.18; F, 12.08%).

4.4.6. 1,2-Dibromo-3,6-difluoro-4,5-dihexyloxybenzene (9). 1,4-Difluoro-2,3-dihexyloxybenzene (**8**, 8.69 g, 0.0276 mol) was stirred in anhydrous dichloromethane (100 ml) at 0°C. The reaction vessel was fitted with a trap containing sodium hydroxide and nitrogen was bubbled through the reaction mixture to remove the HBr produced. Elemental bromine (3.27 ml, 10.21 g, 0.0638 mol, 2.1 eq) in dichloromethane (100 ml) was added drop wise from an addition funnel over 1 hour. After addition was complete, stirring was continued at room temperature overnight. Saturated sodium metabisulphate solution (100 ml) was added and the product was extracted with dichloromethane (2×50 ml). The combined organic extracts were washed with water, dried with magnesium sulphate and filtered. Removal of the solvent *in vacuo* yielded a brown oil. Filtration through a short silica column using 1:1 toluene:dichloromethane as eluant removed the coloured impurities. The solvent was removed *in vacuo* to yield 1,2-dibromo-3,6-difluoro,4,5-dihexyloxybenzene (**6**) as a colourless oil (13.5 g, 97.8%); (found: C, 45.9; H, 5.8. $C_{18}H_{26}O_2F_2Br_2$ requires C, 45.78; H, 5.55; O, 6.78; F, 8.05; Br, 33.84%).

4.4.7. 3',6'-Difluoro-3,4,4',5',3'',4''-hexakishexyloxy [1,1':2',1'']terphenyl (11). 1,2-Dibromo-3,6-difluoro-4,5-dihexyloxybenzene (**9**, 0.5 mmol.) and $Pd(PPh_3)_4$ (3 mol% Pd(0), per bromine atom) were stirred in degassed DME (50 ml) under argon. The pinacol boronate ester (3,4-dihexyloxybenzene boronic acid, 10, 1.5 mmol) was dissolved in toluene, degassed, and after about 15 minutes was added to the reaction by canular. A suspension of barium hydroxide (1.5 mmol.) in water (2.5 ml) was degassed and added directly to the reaction. The reaction was carried out under argon at 80°C, for 21 hours, and then allowed to cool, water was added. The mixture was extracted with ether, the extracts were washed with saturated sodium chloride solution (2×50

ml), water (2×50 ml), dried (Na_2SO_4), and the solvent removed *in vacuo* to leave a red, viscous oil (~80 %). This was subjected to column chromatography on silica gel using petroleum ether/ethyl acetate as the eluting solvent (using a gradient of 9:1 initially to 4:1 finally) (found: C, 74.65; H, 9.8;. $C_{54}H_{84}O_6F_2$ requires: C, 74.79; H, 9.76; O, 11.07; F, 4.38%).

4.4.8. 1,4-Difluoro-2,3,6,7,10,11-hexakis(hexyloxy)triphenylene. 2F-HAT6 (1a). 3',6'-difluoro-3,4,4',5',3'',4''-hexakishexyloxy[1,1':2',1'']terphenyl (11, 0.5 mmol) was stirred in dry CH_2Cl_2 (50 ml). Iron (III) chloride (1 mmol) was weighed and added to the reaction flask under an inert atmosphere. The reaction mixture turned a deep green color and was stirred at room temperature until no starting material remained [TLC (1:1 dichloromethane/ petroleum spirit) on small portions following methanol work up]. The reaction mixture was worked up by pouring onto methanol (anhydrous, 50 ml). To the resulting, brown solution, was added water (50 ml) and DCM (50 ml). The layers were extracted with DCM, washed with ferrous ammonium sulfate (5% solution, 50 ml) and water (2×50 ml). Drying over $MgSO_4$, filtration and removal of solvent *in vacuo* yielded a red to purple solid. The purple solid was dissolved in DCM and filtered through a bed of silica, removal of solvent yielded a sticky off-white solid. The product was recrystallized from ethanol and dried in glass (Yield > 90%). (found: C, 74.7; H, 9.7;. $C_{54}H_{84}O_6F_2$ requires: C, 74.96; H, 9.76; O, 11.07; F, 4.38%); δ_H(300 MHz; $CDCl_3$) 0.9286 (18 H, *t*, *J* = 7 Hz, 6×-Me), 1.380 (24 H, *m*, 12×-CH_2-), 1.57 (12 H, *m*, 6×-$CH_2CH_2CH_2$O-Ar), 1.860 (4 H, quint, *J* = 7 Hz, 2×-$CH_2CH_2CH_2$O-Ar), 1.918 (8 H, quint, *J* = 7 Hz, 4×-$CH_2CH_2CH_2$O-Ar), 4.19 (4 H, *t*, *J* = 7 Hz, 2×-CH_2CH_2O-Ar), 4.224 (8 H, *t*, *J* = 7 Hz, 4×-CH_2CH_2O-Ar), 7.81 (H_b, 2 H, *s*), 8.47 (H_a, 2 H, *t*, *J* = 3.01 Hz, nOe coupling to ^{19}F); 14.07 (6×CH_3), 22.66 (6×CH_2), 25.58 (2×CH_2), 25.81 (4×CH_2), 29.23 (2×CH_2), 29.33 (4×CH_2), 30.21 (2×CH_2), 31.66 (2×CH_2), 31.68 (2×CH_2), 69.06 (2×CH_2OAr), 69.50 (2×CH_2OAr), 75.14 (2×CH_2OAr) 106. 70 (CH, *s*, $C_{8,9}$), 111.43 (CH, m, nOe coupling to ^{19}F, $C_{5,12}$,,), 115.49 (C, *m*, $C_{4a,12b}$), 120.68 (C, *s*, $C_{4b,11a}$), 124.84 (C, *s*, $C_{8a,8b}$), 139.44 (C, *m*, $C_{2,3}$), 148.53 (C, *s*, $C_{7,10}$), 149.14 (C, *s*, $C_{6,11}$), 152.40 [C, *m*, (low intensity), $C_{1,4}$]; m/z (FAB+) 866 (M^+, 100%).

Acknowledgements

We thank the EPSRC, NEDO and the Leverhulme Trust for funding.

References

1. R.J. Bushby and O.R. Lozman, "Photoconducting liquid crystals", *Curr. Opin. Solid State Mater. Sci*. **6**, 569–578 (2002).
2. M. Funahashi and J. Hanna, "Photoconductive smectic liquid crystals and their application to opto-electronic devices", *J. Syn. Org. Chem. Jpn*. **58**, 887–892 (2000).
3. P.M. Borsenberger and D.S. Weiss, *Organic Photoreceptors for Xerography*, Marcel Decker, New York, 1998.
4. C.W. Tang and S.A. van Slyke, "Organic electroluminescent diodes", *Appl. Phys. Lett*. **51**, 913–915 (1987).
5. N. Boden and B. Movaghar, "Applicable properties of columnar discotic liquid crystals", in *Handbook of Liquid Crystals;* Vol. 2B, pp. 781–798, edited by D. Demus, J. Goodby, G.W. Gray, H.W. Spiess, and V. Vill, Wiley, Weinheim, 1998.
6. K. Kawata, "Orientation control and fixation of discotic liquid crystals", *Chem. Rec*. **2**, 59–80 (2002).
7. R.J. Bushby and A.N. Cammidge, "Discotic liquid crystals – synthesis and structural features", in *Handbook of Liquid Crystals*, Vol. 2B, pp. 693–748, edited by D. Demus, J. Goodby, G.W. Gray, H.W. Spiess and V. Vill, Wiley, Weinheim, 1998.
8. R.J. Bushby, N. Boden, C.A. Kilner, O.R. Lozman, Z, Lu, Q. Liu and M.A. Thornton-Pett, "Helical geometry and liquid crystalline properties of 2,3,6,7,10,11-hexaalkoxy-1-nitrotriphenylenes", *J. Mater. Chem*. **13**, 470–474 (2003).
9. C.Y. Liu, A. Fechtenkotter, M.D. Watson, K. Mullen, and A.J. Bard, "Room temperature discotic liquid crystalline thin films of hexa-peri-hexabenzocoronene: Synthesis and optoelectronic properties", *Chem. Mater.* **15**, 124–130 (2003).
10. O. Arikainen, N. Boden, R.J. Bushby, O.R. Lozman, J.G. Vinter, and A. Wood, "Complementary polytopic interactions", *Angew. Chem*. **39**, 2333–2336 (2000).
11. N. Boden, R.J. Bushby, G. Cooke, O.R. Lozman and Z. Lu, "CPI: A recipe for improving applicable properties of discotic liquid crystals", *J. Amer. Chem. Soc*. **123**, 7915–7916 (2001).
12. O.R. Lozman, "Self-assembly of disc shaped molecules", *PhD Thesis*, Leeds, 2000.
13. N. Boden, R.J. Bushby, A.N. Cammidge, and G. Headdock, "Versatile synthesis of unsymmetrically substituted triphenylenes", *Synthesis* **6**, 31–32 (1995).
14. N. Boden, R.J. Bushby, G. Headdock, O.R. Lozman, and A. Wood, "Synthesis of large core discogens based on the triphenylene, azatriphenylene and hexabenztrinaphthalene nuclei", *Liq. Cryst*. **28**, 139–144 (2001).
15. N. Boden, R.C. Borner, R.J. Bushby, A.N. Cammidge, and M.V. Jesudason, "The synthesis of triphenylene based discotic mesogens: New and improved routes", *Liq. Cryst*. **15**, 851–858 (1993).
16. N. Miyaura and A. Suzuki, "Palladium-catalysed cross-coupling reactions of organoboron compounds", *Chem. Rev*. **95**, 2457 (1995).
17. O.R. Lozman, R.J. Bushby, and J.G. Vinter, "Complementary polytopic interactions (CPI) as revealed by molecular modelling using the XED force field", *J. Chem. Soc*., *Perkin Trans*. **2**, 1446–1452 (2001).
18. J. Simmerer, B. Glusen, W. Paulus, A. Kettner, P. Schuhmacher, D. Adam, K.H. Etzbach, K. Siemensmeyer, J.H. Wendorff, H. Ringsdorf, and D. Haarer, "Transient photoconductivity in a discotic hexagonal plastic crystal", *Adv. Mater.* **8**, 815 (1996).
19. D. Adam, P. Schuhmacher, J. Simmerer, L. Haussling, K. Siemensmeyer, K.H. Etzbach, H. Ringsdorf, and D. Haarer, "Fast photoconduction in the highly ordered columnar phase of a discotic liquid-crystal", *Nature* **371**, 141 (1994).

20. D. Adam, F. Closs, T. Frey, D. Funhoff, D. Haarer, H. Ringsdorf, P. Schuhmacher, and K. Siemensmeyer, "Transient photoconductivity in a discotic liquid-crystal", *Phys. Rev. Lett.* **70**, 457–460 (1993).
21. N. Boden, R.J. Bushby, A.N. Cammidge, J. Clements, R. Luo, and K.J. Donovan, "Transient photoconductivity and dark conductivity in discotic liquid crystals", *Mol. Cryst. Liq. Cryst.* **261**, 251–257 (1995).
22. T. Kreouzis, K.J. Donovan, N. Boden, R.J. Bushby, O.R. Lozman, and Q Liu, "Temperature-independent hole mobility in discotic liquid crystals", *J. Chem. Phys.* **114,** 1797–1802 (2000).
23. N. Boden, R.J. Bushby, and J. Clements, "Mechanism of quasi-one-dimensional electronic conductivity in discotic liquid crystals", *J. Chem. Phys.* **98**, 5920–5931 (1993).
24. N. Boden, R.J. Bushby, J. Clements, B. Movhagar, K.J. Donovan, and T. Kreouzis, "Mechanism of charge transport in discotic liquid crystals", *Phys. Rev.* **B52**, 13274–13280 (1995).
25. V. Lemaur, D.A. Da Silva Filho, V. Coropceanu, M. Lehmann, Y. Geerts, J. Piris, M.G. Debije, A.M. van de Craats, K. Senthilkumar, L.D.A. Siebbeles, J.M. Warman, J.L. Bredas, and J. Cornil, "Charge transport properties in discotic liquid crystals: A quantum-chemical insight into structure-property relationships", *J. Amer. Chem. Soc.* **126**, 3271–3279 (2004).
26. A.M. van de Craats and J.M. Warman, "The core-size effect on the mobility of charge in discotic liquid crystalline materials", *Adv. Mater.* **13**, 130–133 (2001).
27. K. Senthilkumar, F.C. Grozema, F.M. Bickelhaupt, and L.D.A. Siebbeles, "Charge transport in columnar stacked triphenylenes: Effects of conformational fluctuations on charge transfer integrals and site energies", *J. Chem. Phys.* **119**, 9809–9817 (2003).
28. E.O. Arikainen, N. Boden, R.J. Bushby, J. Clements, B. Movaghar, and A. Wood, "Effects of side-chain length on the charge transport properties of discotic liquid crystals and their implications for the charge transport mechanism", *J. Mater. Chem.* **5**, 2161–2165 (1995).
29. P.M. Borsenberger and M.B. O'Regan, "The role of dipole-moment on hole transport in tiphenylamine doped poly(styrene)", *Chem. Phys.* **200**, 257–262 (1995).
30. A. Ochse, A. Kettner, J. Kopitzke, W.H. Wendorff and H. Bassler, "Transient photoconduction in discotic liquid crystals", *Phys. Chem. Chem. Phys.* **1**, 1757–1760 (1999).
31. R.J. Bushby, O.R. Lozman, L.A. Mason, and N. Taylor, "Cyclic voltammetry studies of discotic liquid crystals", *Mol. Cryst. Liq. Cryst.* **410**, 699–709 (2004).
32. B.R. Wegewijs, L.D.A. Siebbeles, N. Boden, R.J. Bushby, B. Movaghar, O.R. Lozman, Q. Liu, A. Pecchia, and L.A. Mason, "Charge-carrier mobilities in binary mixture discotic triphenylene derivatives as a function of temperature", *Phys. Rev.* **B65**, 245112 (2002).
33. K.J. Donovan, K. Scott, S. Spagnoli, and J. Berrehar, "DC photoconduction action spectra in thin film polymer crystals of 3 and 4BCMU polydiacetylene", *Chem. Phys.* **250**, 61–70 (1999).
34. K.J. Donovan and T. Kreouzis, "Deconvolution of time of flight photocurrent transients and electronic response time in columnar liquid crystals", *J. Appl. Phys.* **88**, 918–923 (2000).
35. XED v5.52 (C) Cresset Biomolecular Discovery Ltd.
36. K. Praefcke, A. Eckert, and D. Blunk, "Core-halogenated, helical-chiral triphenylene-based columnar liquid crystals", *Liq. Cryst.* 22, 113–119 (1997).
37. T. Kreouzis, K. Scott, K.J. Donovan, N. Boden, R.J. Bushby, O.R. Lozman, and Q. Liu, "Enhanced electronic transport properties in complementary binary discotic liquid crystal systems", *Chem. Phys.* **262**, 489–497 (2000).

CALL FOR PAPERS

Be a part of the leading event for photonics research and applications—submit your abstracts today.

Photonics WEST

21–26 January 2006
San Jose, California USA

Share your research with your colleagues. Submit your paper to these four major SPIE International Symposia.

- BiOS 2006—International Biomedical Optics Symposium
- LASE 2006—Lasers and Applications in Science and Engineering
- Optoelectronics 2006—Integrated Optoelectronic Devices
- MOEMS-MEMS 2006—Micro & Nanofabrication

If selected, your editor-reviewed paper will be published in the SPIE Digital Library just 2 to 4 weeks after the conference. No other publisher today has editor-reviewed research online as quickly. In a world where science and technology knowledge increases daily, timing matters.

Your participation adds to the critical mass of knowledge and furthers the global impact of these technologies.

SPIE The International Society for Optical Engineering

SPIE—The International Society for Optical Engineering is a not-for-profit technical education society dedicated to advancing scientific research and engineering applications of optical, photonic, imaging, and optoelectronic technologies through its meetings, education programs, and publications.

spie.org | spie@spie.org | Tel: +1 360 676 3290
1000 20th St, Bellingham WA, 98225-6705 USA

